Systematic study of the fusion barriers using different proximity-type potentials for $N = Z$ colliding nuclei: New extensions

Ishwar Dutt and Rajeev K. Puri[*]

Department of Physics, Panjab University, Chandigarh 160 014, India

By using 14 different versions and parametrizations of a proximity potential and two new versions of the potential proposed in this paper, we perform a comparative study of fusion barriers by studying 26 symmetric reactions. The mass asymmetry $\eta_A = (\frac{A_2 - A_1}{A_2 + A_1})$, however, is very large. Our detailed investigation reveals that most of the proximity potentials reproduce experimental data within $\pm 8\%$ on average. A comparison of fusion cross sections indicates that Bass 80, AW 95, and Denisov DP potentials have a better edge than other potentials. We also propose new versions of the proximity potential as well as Denisov parametrized potential. These new versions improve agreement with the data.

I. INTRODUCTION

The study of fusion barriers and fusion cross sections has received renewed attention in recent years [1–5]. This renewed interest is caused by the efforts of low and intermediate energies in order to understand the fusion mechanism and, subsequently, the nucleus-nucleus interactions in nuclear physics. This is further boosted by the availability of radioactive-ion beams involving various reactions [5].

In recent years, large numbers of models depending on the vast variety of assumptions have been proposed [1,3,4,6–10]. One set of such theoretical models is based on the microscopic picture in which one starts from two- and three-body effective interactions and calculates the ion-ion potential [3,4,9]. Another class of models takes the gross macroscopic picture into account [11,12]. Because of the recent precise measurements of the fusion cross sections, the job of theoretical models has become much more complex. Among different theoretical models, the proximity potential enjoys special status [6,7]. All proximity potentials are based on the proximity force theorem, according to which the nuclear part of the interaction potential can be written as the product of a factor depending on the mean curvature of the interaction surface and a universal function (depending on the separation distance) and is independent of the masses of colliding nuclei. This concept did introduce a great amount of simplification in nuclear potential studies [4,9]. Several refinements and modifications have been proposed in the recent past concerning the original proximity potential to remove the gray part of the potential [6]. This observation demands a careful and systematic study of the heavy-ion fusion process using all such potentials that are remodeled and parametrized within the proximity concept.

Here, we will concentrate on the symmetric colliding pairs with symmetry parameter $A_s = (\frac{N-Z}{A}) = 0.0$ only. Here, N and Z belong to the combined neutron and proton content of the reaction. This comparison, which covers a wide spectrum, will give us a unique possibility to compare various modeled proximity potentials. We also plan to modify the proximity potential and the potential by Denisov and we will show that

these new versions improve agreement with the experimental data. Section II describes the Formalism in brief, Sec. III depicts the results and Summary is presented in Sec. IV.

II. FORMALISM

According to the original version of the proximity potential 1977 [7], the interaction potential $V_N(r)$ between two surfaces can be written as

$$V_N^{\text{Prox } 77}(r) = 4\pi\gamma b\overline{R}\Phi(r - C_1 - C_2/b)\text{MeV}, \quad (1)$$

where γ is the surface energy coefficient. The mean curvature radius $\overline{R}$ in Eq. (1) is written as

$$\overline{R} = C_1 C_2/(C_1 + C_2), \quad C_i = R_i[1 - (b/R_i)^2 + \cdots], \quad (2)$$

and R_i, the effective sharp radius, reads as

$$R_i = 1.28 A_i^{1/3} - 0.76 + 0.8 A_i^{-1/3} \text{fm} \quad (i = 1, 2). \quad (3)$$

This model is referred to as Prox 77, and the corresponding potential is referred to as $V_N^{\text{Prox } 77}(r)$.

Later, Reisdorf [8] modified the preceding potential with a different γ value. This is labeled as Prox 88.

The latest version of the proximity potential by Myers and Świątecki (labeled here as Prox 00) is given in Ref. [6]. This Prox 00 uses an experimental value and/or an old formula for the radius.

Recently, Royer and Rousseau [2] gave a more precise radius formula

$$R_i = \alpha A_i^{1/3}(1 + \beta/A_i - \delta A_{si}) \text{fm} \quad (i = 1, 2), \quad (4)$$

where α, β, and δ are constants that have values of 1.2332, 2.348 443, and 0.151 541, respectively. This formula is obtained by analyzing as many as 2027 masses with $N, Z \geqslant 8$, and a mass uncertainty $\leqslant 150$ keV. We implement this radius formula in Prox 00 and label it as Prox 00DP.

Based on the proximity concept, many other potentials have also been shown in the literature. We will use the potentials by Bass (labeled here as Bass 73 [11], similarly, Bass 77 [12], and Bass 80 [8]), Christensen and Winther (CW 76) [13] Broglia and Winther (BW 91) [8], Aage Winther (AW 95) [10],

---

Ngô *et al.* (Ngô 75) [14], Ngô and Ngô (Ngô 80) [15], and Denisov [9].

The potential by Denisov [9] is also modified here to include the previous more precise radius formula [Eq. (4)] in its parametrization. This is labeled as Denisov DP.

The exact potential based on the Skyrme energy density formalism (labeled as EDF Exact) [3] along with its parametrized form (labeled as EDF Par) [16] will also be used for comparison. Note that Skyrme forces are also widely used in intermediate energies [17].

III. RESULTS AND DISCUSSION

In Fig. 1, we display the nuclear part of the interaction potential V_N(MeV) as a function of internuclear distance r (in femtometers) using some of the previously listed versions of the proximity potentials for the reactions of $^{16}O + ^{16}O$ and $^{40}Ca + ^{40}Ca$. In Fig. 1(a), we display three versions of the potentials by Bass, whereas in Fig. 1(b) we deal with Ngô parametrizations. The potentials of Winther and collaborators are displayed in Fig. 1(c), followed by four versions of a proximity potential displayed in Fig. 1(d).

From the figure, we see that different versions of the Bass potentials as well as the CW 76 do not have a repulsive core at a shorter distance. On the other hand, the BW 91 and AW 95 potentials follow the Woods-Saxon-type distributions. All other potentials have acceptable shapes: that is, attractive
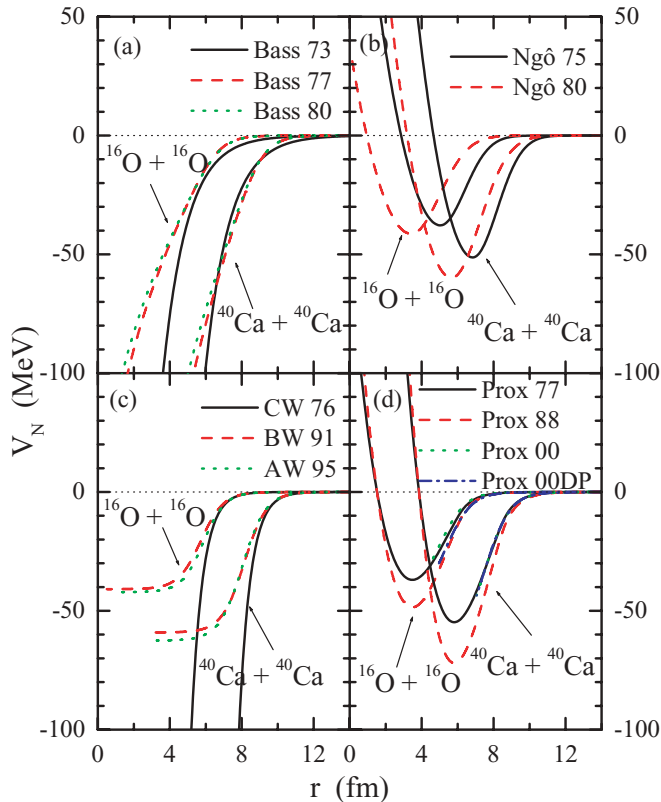
at long distances followed by repulsive at shorter distances. Interestingly, the deepest potential is caused by the proximity potential Prox 88 (=72 MeV). In other words, one can see a huge difference in the potentials obtained from different versions of the proximity-based formalisms even within the same model. For instance, different versions of the proximity potential differ by as much as 17 MeV for the reaction of $^{40}Ca + ^{40}Ca$. Since the fusion process is a low-density phenomenon happening at the outer surface, the difference in the inner part of the potential may not be so important. By adding the Coulomb potential to the nuclear part, one can compute the total potential $V_T(r)$ as

$$V_T(r) = V_N(r) + V_C(r) \tag{5}$$

$$= V_N(r) + \frac{Z_1 Z_2 e^2}{r}. \tag{6}$$

Since the fusion happens at a distance greater than the touching configuration of the colliding pair, the previous form of the Coulomb potential is justified. One can extract the barrier height V_B^{theor} and the barrier position R_B^{theor} using the following conditions:

$$\left.\frac{dV_T(r)}{dr}\right|_{r=R_B^{\text{theor}}} = 0 \quad \text{and} \quad \left.\frac{d^2V_T(r)}{dr^2}\right|_{r=R_B^{\text{theor}}} \leqslant 0. \tag{7}$$

In Fig. 2, we display the total interaction (nuclear + Coulomb) potential V_T(MeV) as a function of internuclear distance r (in femtometers). We display the results using different versions of the proximity potentials (Prox 77, Prox 88, Prox 00, and Prox 00DP) and the potentials of Winther and collaborators (i.e., CW 76, BW 91, and AW 95). From Fig. 2,
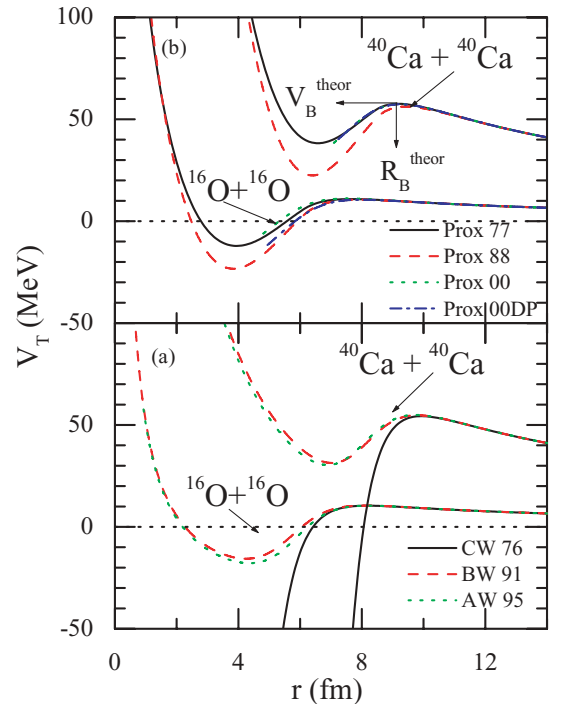

FIG. 1. (Color online) The nuclear part of the interaction potential V_N(MeV) as a function of internuclear distance r (in femtometers) for the reactions of $^{16}O + ^{16}O$ and $^{40}Ca + ^{40}Ca$ using different proximity potentials.

FIG. 2. (Color online) The total interaction potential V_T(MeV) as a function of internuclear distance r (in femtometers). Here, we display the results obtained with different versions of proximity and Winther potentials only.
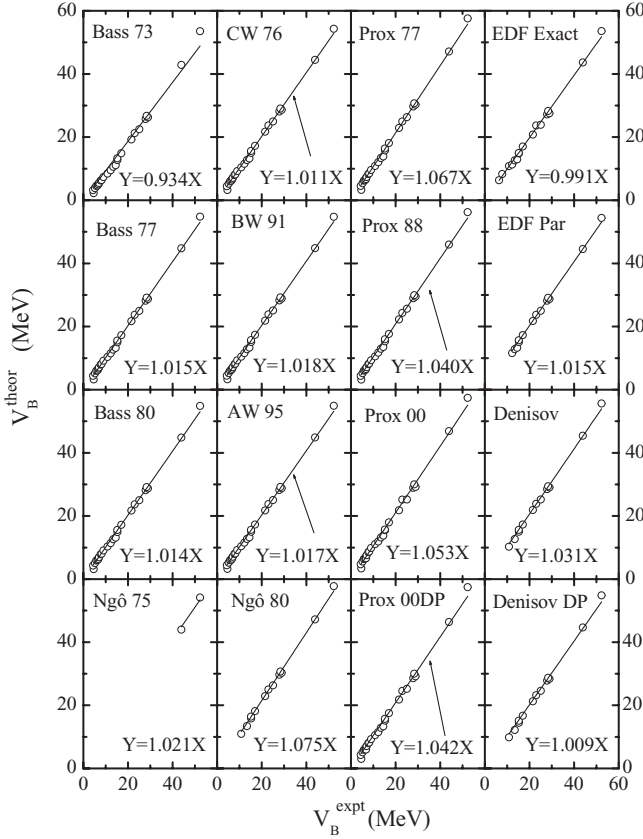
FIG. 3. Comparison of theoretical fusion barrier heights V_B^{theor}(MeV) using different proximity potentials with experimental values V_B^{expt}(MeV) [19–25]. The solid lines represent the straight-line least-squares fit created over different points.

we note that, although various potentials differ significantly in the interior part, very little dependence is visible on the surface part and on the barrier region. In terms of fusion barrier heights and positions, all versions yield nearly the same barrier heights and positions. Of course, the shape and the curvature of the potential differs, indicating a different picture for subbarrier fusion cross sections that depends sensitively on the shape of the potential one is using. For the reaction of ^{40}Ca + ^{40}Ca, no difference is seen between Prox 00 and Prox 00DP. This happens because the experimental value of the charge distribution is available for the ^{40}Ca nucleus, and both models use the same experimental values. The results may differ for those nuclei in which experimental values are not available.

Knowledge of the shape of the potential, as well as the barrier position and the height, allows one to calculate the fusion cross section at a microscopic level. To study the fusion cross sections, we will use the model given by Wong [18]. In this formalism, the cross section for complete fusion is given by

$$\sigma_{\text{fus}} = \frac{\pi}{k^2} \sum_{l=0}^{l_{\max}} (2l + 1) T_l(E_{\text{cm}}), \qquad (8)$$

where $k = \sqrt{2\mu E/\hbar^2}$ and here μ is the reduced mass. The center-of-mass energy is denoted by E_{cm}. In this formula, $l_{\max}$ corresponds to the largest partial wave for which a pocket

still exists in the interaction potential, and $T_l(E_{\text{cm}})$ is the energy-dependent barrier penetration factor and is given by

$$T_l(E_{\text{cm}}) = \left\{ 1 + \exp\left[\frac{2\pi}{\hbar\omega_l} \left(V_{B_\ell}^{\text{theor}} - E_{\text{cm}} \right) \right] \right\}^{-1}, \qquad (9)$$

where $\hbar\omega_l$ is the curvature of the inverted parabola. If we assume that the barrier position and the width are independent of l, the fusion cross section reduces to

$$\sigma_{\text{fus}}(\text{mb}) = \frac{10 R_B^{\text{theor}^2} \hbar\omega_0}{2 E_{\text{cm}}}$$
$$\times \ln\left\{ 1 + \exp\left[\frac{2\pi}{\hbar\omega_0} \left(E_{\text{cm}} - V_B^{\text{theor}} \right) \right] \right\}. \qquad (10)$$

For $E_{\text{cm}} \gg V_B^{\text{theor}}$, the preceding formula reduces to a well-known sharp cutoff formula

$$\sigma_{\text{fus}}(\text{mb}) = 10\pi R_B^{\text{theor}^2} \left(1 - \frac{V_B^{\text{theor}}}{E_{\text{cm}}} \right), \qquad (11)$$

whereas for $E_{\text{cm}} \ll V_B^{\text{theor}}$, the foregoing formula reduces to

$$\sigma_{\text{fus}}(\text{mb}) = \frac{10 R_B^{\text{theor}^2} \hbar\omega_0}{2 E_{\text{cm}}} \exp\left[\frac{2\pi}{\hbar\omega_0} \left(E_{\text{cm}} - V_B^{\text{theor}} \right) \right]. \qquad (12)$$

We used Eq. (10) to calculate the fusion cross sections.

In Fig. 3, we display the theoretical barrier heights V_B^{theor}(MeV) versus the experimental barrier heights V_B^{expt}(MeV) using all 16 different potentials. The experimental barrier heights V_B^{expt} are taken directly from the literature [19–25]. The limited numbers of reactions in certain cases
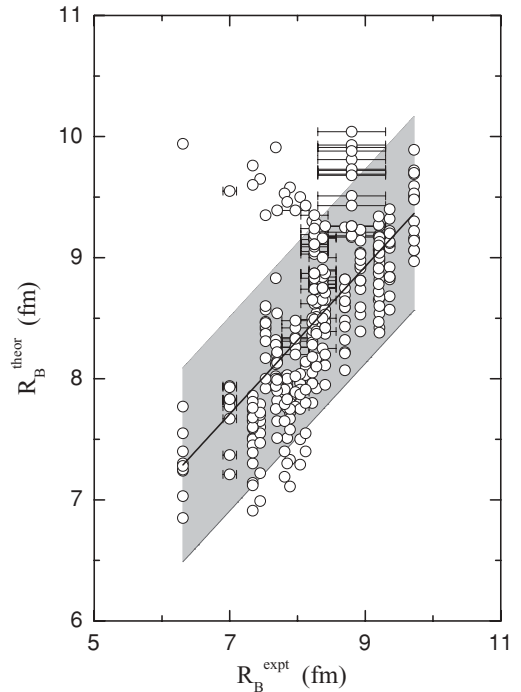

FIG. 4. A comparison of theoretical R_B^{theor}(fm) and experimental fusion barrier positions R_B^{expt}(fm) [19–25] using various versions of the proximity potential. Solid lines represent the straight-line least-squares fit.
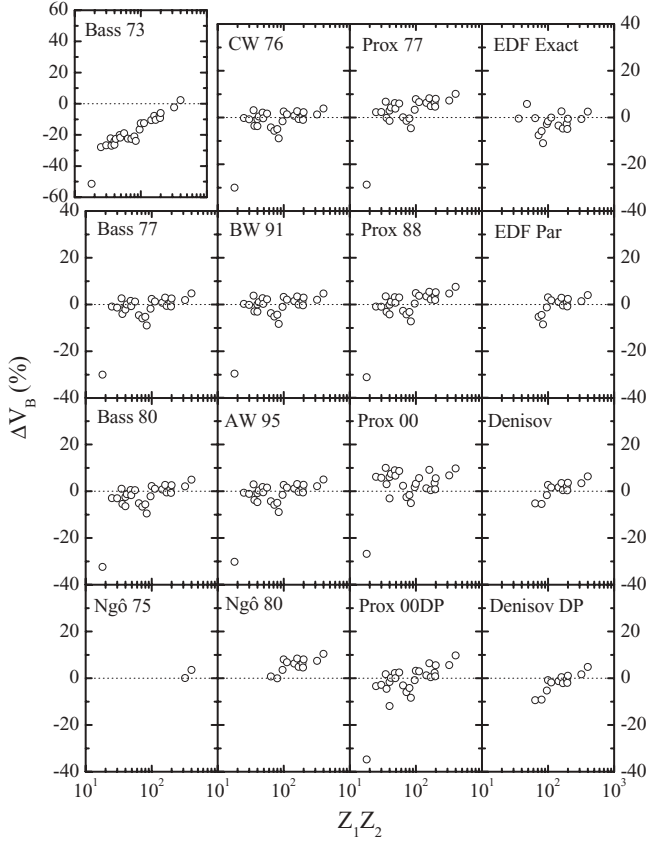
FIG. 5. The percentage deviation $\Delta V_B(\%)$ as a function of the product of charges $Z_1 Z_2$ using different versions of the proximity potential.

are caused by the restrictions posed on different potentials [3,9,14–16]. The lines are the fits over the points. These fitted equations distinguish the deviation from the experimental data. Very interestingly, we see that all models can reproduce the experimental barrier heights for symmetric colliding nuclei within ±8% on average. We also notice that, on average, barriers formed using EDF Exact, EDF Par, Bass 77, Bass 80, Denisov DP, and the different versions by Winther and collaborators are close to the experimental data. On the other hand, barriers formed within Bass 73, Ngô 80, and Prox 77 potentials deviate by ±7% from the experimental values. The revised versions by Bass improve the barrier heights drastically. Now, Bass 77 and Bass 80 reproduce the experimental data within 1.5%. A newer version of the Bass potential (Bass 80) shows slight improvement over Bass 77. Strangely, the Ngô 80 version deviates more than 7%, whereas its first version was able to reproduce the barrier within 2%. For Ngô 75, only two systems fall within its parametrization limits.

The four versions of the proximity potentials yield an interesting comparison. As pointed out by various authors [6], Prox 77 deviates from the experimental fusion barrier heights by 4% (here, it is 6.73%), whereas the new versions of the proximity potential results are lowered to 0.01% (here, it is 5.34%). Note that in Ref. [6], very old data for the fusion barrier were used. In this paper, we have used the latest data. It is worth mentioning that a slight variation in the radius formula (Prox 00 and Prox 00DP) can improve the comparison

by nearly 1%. Very interestingly, a change in the value of the surface energy coefficient γ (Prox 77 and Prox 88) improves agreement drastically [26]. Further, the advantage of a new proximity potential (Prox 00) can clearly be obtained by just using γ in Prox 77 as suggested by Reisdorf [8]. We do not see a direct advantage of the original Denisov form of the potential over the Skyrme energy density model by Puri and Gupta [16] in which a perfect comparison with the experimental data is clearly visible. Its new form, Denisov DP, however, shows perfect agreement with the experimental data. From these figures and this analysis, it is very clear that different models do not yield very different results. Instead, technical parameters, such as the surface energy coefficient γ and the radius, can have a significant impact on the outcome. The implementation of the latest radius formula clearly yields better agreement.

In Fig. 4, we display the fusion barrier positions as a function of experimentally extracted values. We see that no trend emerges in this case. This happens because of a great amount of uncertainty in the measurement of the fusion barrier positions reported by various authors in various experiments [20,21].

In Fig. 5, we display the percentage difference of the fusion barrier heights over its experimental values defined as

$$\Delta V_B(\%) = \frac{V_B^{\text{theor}} - V_B^{\text{expt}}}{V_B^{\text{expt}}} \times 100. \qquad (13)$$

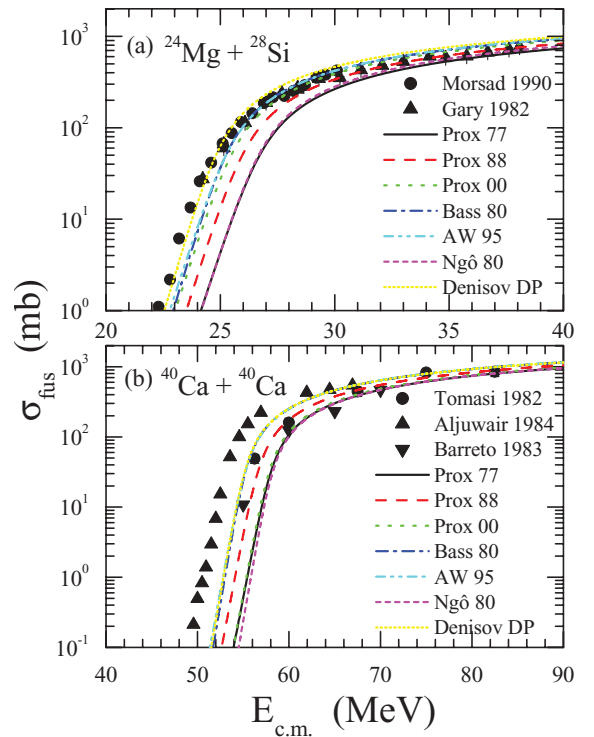We see that, on an individual basis, all proximity potentials can reproduce the data within ±10%. The least amount of

FIG. 6. (Color online) The fusion cross sections for the reactions of ^{24}Mg + ^{28}Si [Fig. 6(a)] and ^{40}Ca + ^{40}Ca [Fig. 6(b)] as a function of center-of-mass energy E_{cm}. The experimental data are taken from Morsad 1990 [22], Gary 1982 [23], Tomasi 1982 [24], Aljuwair 1984 [21], and Barreto 1983 [25]. For the clarity, only the latest versions of the different proximity potentials are shown.

deviation is attained from Bass 77, Bass 80, different Winther potentials (CW 76, BW 91, and AW 95), EDF Exact, EDF Par, and Denisov DP (all within $\pm 5\%$). However, the proximity potential (Prox 77) deviates much more compared to its other versions.

In Fig. 6, we display the fusion cross section σ_{fus} (in millibarns) as a function of center-of-mass energy E_{cm} for the reactions of $^{24}\text{Mg} + ^{28}\text{Si}$ [Fig. 6(a)] and $^{40}\text{Ca} + ^{40}\text{Ca}$ [Fig. 6(b)]. Here, the latest versions of the proximity parametrizations along with the original proximity potential and its modifications are shown for clarity. The experimental data are taken from Refs. [21–25]. As we see, Bass 80, Denisov DP, and AW 95 do a better job for the reaction of $^{24}\text{Mg} + ^{28}\text{Si}$, whereas Prox 77 and Ngô 80 fail to come close to the experimental data. For the reaction of $^{40}\text{Ca} + ^{40}\text{Ca}$, no clear picture emerges. In both cases, the potentials of Denisov DP and AW 95 are able to reproduce the cross section.

IV. SUMMARY

By using as many as 16 versions of the proximity potential derived either from the proximity potential or from the parametrized versions in terms of the proximity concept, we carried out a comparative study of fusion barriers for symmetric colliding nuclei. For the present study, four versions of the proximity potential, three versions of the proximity potential by Bass, three versions of the proximity potentials by Winther and collaborators, two versions of the proximity potentials by Ngô and co-workers, and two versions of the proximity potentials by Denisov and EDF each were taken. We also propose new versions of the proximity potential as well as Denisov parametrized potential. A detailed study reveals that all potentials can reproduce experimental data, on average, within $\pm 8\%$. However, the comparison of fusion cross sections reveals that the Bass 80, Denisov DP, and AW 95 potentials reproduce data better than the other potentials.

[1] K. Siwek-Wilczyńska and J. Wilczyński, Phys. Rev. C **69**, 024611 (2004); N. G. Nicolis, Eur. Phys. J. A **21**, 265 (2004).

[2] G. Royer and R. Rousseau, Eur. Phys. J. A **42**, 541 (2009).

[3] R. K. Puri and N. K. Dhiman, Eur. Phys. J. A **23**, 429 (2005); R. Arora, R. K. Puri, and R. K. Gupta, *ibid.* **8**, 103 (2000); J. K. Dhawan, N. K. Dhiman, A. Sood, and R. K. Puri, Phys. Rev. C **74**, 057901 (2006); R. K. Puri, P. Chattopadhyay, and R. K. Gupta, *ibid.* **43**, 315 (1991); N. K. Dhiman and R. K. Puri, Acta Phys. Pol. B **37**, 1855 (2006); **38**, 2133 (2007).

[4] A. Dobrowolski, K. Pomorski, and J. Bartel, Nucl. Phys. A **729**, 713 (2003); N. Wang, X. Wu, Z. Li, M. Liu, and W. Scheid, Phys. Rev. C **74**, 044604 (2006).

[5] L. F. Canto, P. R. S. Gomes, J. Lubian, L. C. Chamon, and E. Crema, Nucl. Phys. A **821**, 51 (2009); A. M. Stefanini *et al.*, Phys. Lett. B **679**, 95 (2009).

[6] W. D. Myers and W. J. Świątecki, Phys. Rev. C **62**, 044610 (2000).

[7] J. Blocki, J. Randrup, W. J. Świątecki, and C. F. Tsang, Ann. Phys. (NY) **105**, 427 (1977).

[8] W. Reisdorf, J. Phys. G **20**, 1297 (1994).

[9] V. Y. Denisov, Phys. Lett. B **526**, 315 (2002).

[10] A. Winther, Nucl. Phys. A **594**, 203 (1995).

[11] R. Bass, Phys. Lett. B **47**, 139 (1973).

[12] R. Bass, Phys. Rev. Lett. **39**, 265 (1977).

[13] P. R. Christensen and A. Winther, Phys. Lett. B **65**, 19 (1976).

[14] C. Ngô, B. Tamain, M. Beiner, R. J. Lombard, D. Mas, and H. H. Deubler, Nucl. Phys. A **252**, 237 (1975).

[15] H. Ngô and C. Ngô, Nucl. Phys. A **348**, 140 (1980).

[16] R. K. Puri and R. K. Gupta, Int. J. Mod. Phys. E **1**, 269 (1992).

[17] S. Kumar, S. Kumar, and R. K. Puri, Phys. Rev. C **78**, 064602 (2008); **81**, 014611 (2010); **81**, 014601 (2010); Y. K. Vermani *et al.*, J. Phys. G **37**, 015105 (2010); Europhys. Lett. **85**, 62001 (2009); Y. K. Vermani, S. Goyal, and R. K. Puri, Phys. Rev. C **79**, 064613 (2009).

[18] C. Y. Wong, Phys. Lett. B **42**, 186 (1972); Phys. Rev. Lett. **31**, 766 (1973).

[19] L. C. Vaz, J. M. Alexander, and G. R. Satchler, Phys. Rep. **69**, 373 (1981); G. M. Berkowitz, P. Braun-Munzinger, J. S. Karp, R. H. Freifelder, T. R. Renner, and H. W. Wilschut, Phys. Rev. C **28**, 667 (1983); R. M. Anjos *et al.*, *ibid.* **49**, 2018 (1994); C. M. Jachcinski *et al.*, *ibid.* **24**, 2070 (1981); D. Shapira *et al.*, *ibid.* **28**, 1148 (1983); J. Skalski, *ibid.* **76**, 044603 (2007); K. Washiyama and D. Lacroix, *ibid.* **78**, 024610 (2008); E. F. Aguilera, J. J. Kolata, P. A. DeYoung, and J. J. Vega, *ibid.* **33**, 1961 (1986); J. Takahashi *et al.*, Phys. Rev. Lett. **78**, 30 (1997).

[20] M. Trotta, A. M. Stefanini, L. Corradi, A. Gadea, F. Scarlassara, S. Beghini, and G. Montagnoli, Phys. Rev. C **65**, 011601(R) (2001).

[21] H. A. Aljuwair *et al.*, Phys. Rev. C **30**, 1223 (1984).

[22] A. Morsad, J. J. Kolata, R. J. Tighe, X. J. Kong, E. F. Aguilera, and J. J. Vega, Phys. Rev. C **41**, 988 (1990).

[23] S. Gary and C. Volant, Phys. Rev. C **25**, 1877 (1982).

[24] E. Tomasi *et al.*, Nucl. Phys. A **373**, 341 (1982).

[25] J. Barreto, G. Auger, M. Langevin, and E. Plagnol, Phys. Rev. C **27**, 1335 (1983).

[26] I. Dutt and R. K. Puri, Phys. Rev. C **81**, 047601 (2010).